

Cell Host & Microbe, Volume 30

Supplemental information

**Antibody escape and cryptic
cross-domain stabilization
in the SARS-CoV-2 Omicron spike protein**

Kamyab Javanmardi, Thomas H. Segall-Shapiro, Chia-Wei Chou, Daniel R. Boutz, Randall J. Olsen, Xuping Xie, Hongjie Xia, Pei-Yong Shi, Charlie D. Johnson, Ankur Annapareddy, Scott Weaver, James M. Musser, Andrew D. Ellington, Ilya J. Finkelstein, and Jimmy D. Gollihar

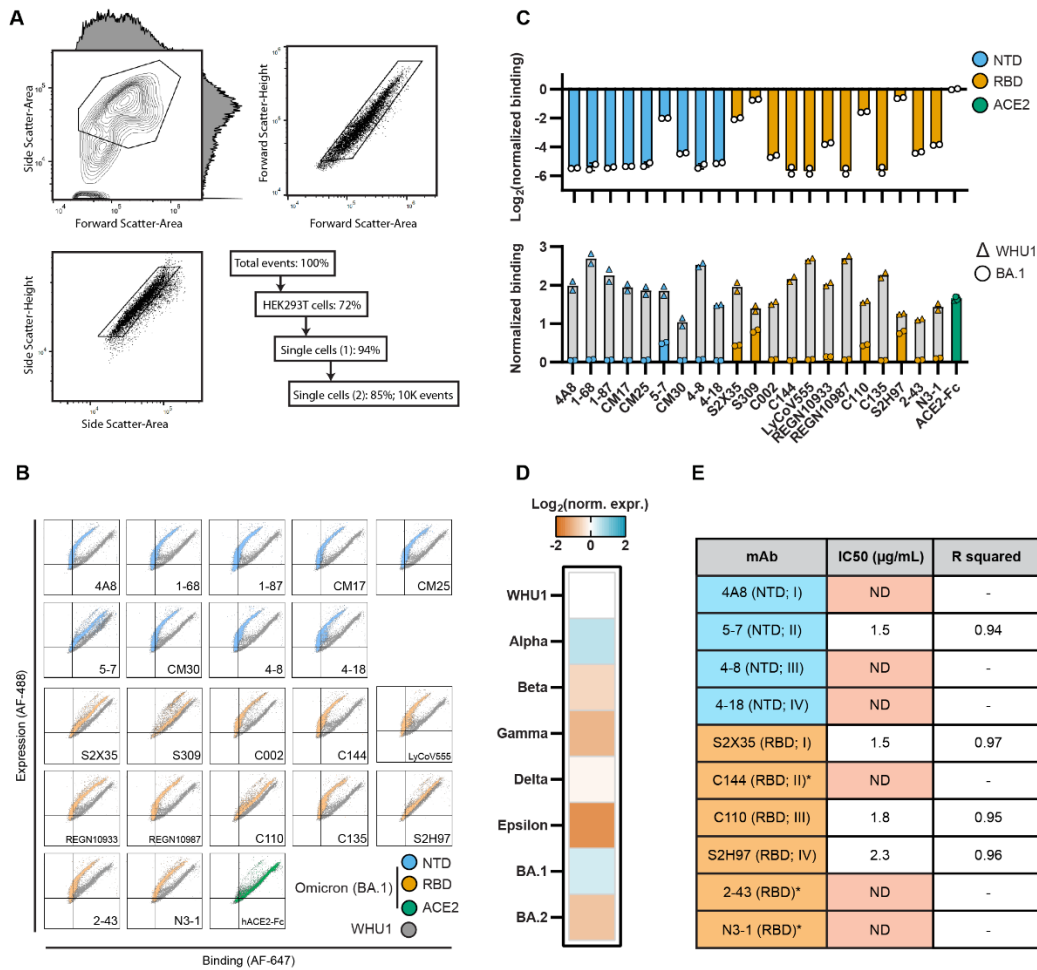


Figure S1. Spike Display enables rapid characterization of spike proteins variants, Related to Figure 1

(A) Flow cytometry gating (shown with data for BA.1 in Figure 1F; STAR Methods).

(B) Representative flow cytometry data for WHU1 spike protein (grey) and BA.1 spike protein (colors) labeled for expression (y-axis) and antibody / ACE2 binding (x-axis). A shift to the left between WHU1 and BA.1 shows reduced antibody / ACE2 binding at the comparable levels of spike protein expression. Median fluorescence values used to calculate normalized binding for each spike protein variant and antibody / ACE2 combination (STAR Methods).

(C) Quantitative data for the BA.1 and WHU1 rows in Figure 1F. Normalized change in binding (top) shows the difference in normalized monoclonal antibody and ACE2 binding between BA.1 and WHU1. Normalized binding (bottom) shows the binding values for these antibodies and ACE2 for both WHU1 (grey) and BA.1 (colors) relative to expression. Bar graphs represent mean \pm SD of log-transformed values from at least two biological replicates.

(D) Relative expression values for the spike protein variants shown in Figure 1F, normalized to WHU1 expression.

(E) IC₅₀ and fit data calculated from the plots shown in Figures 1G and 1H.

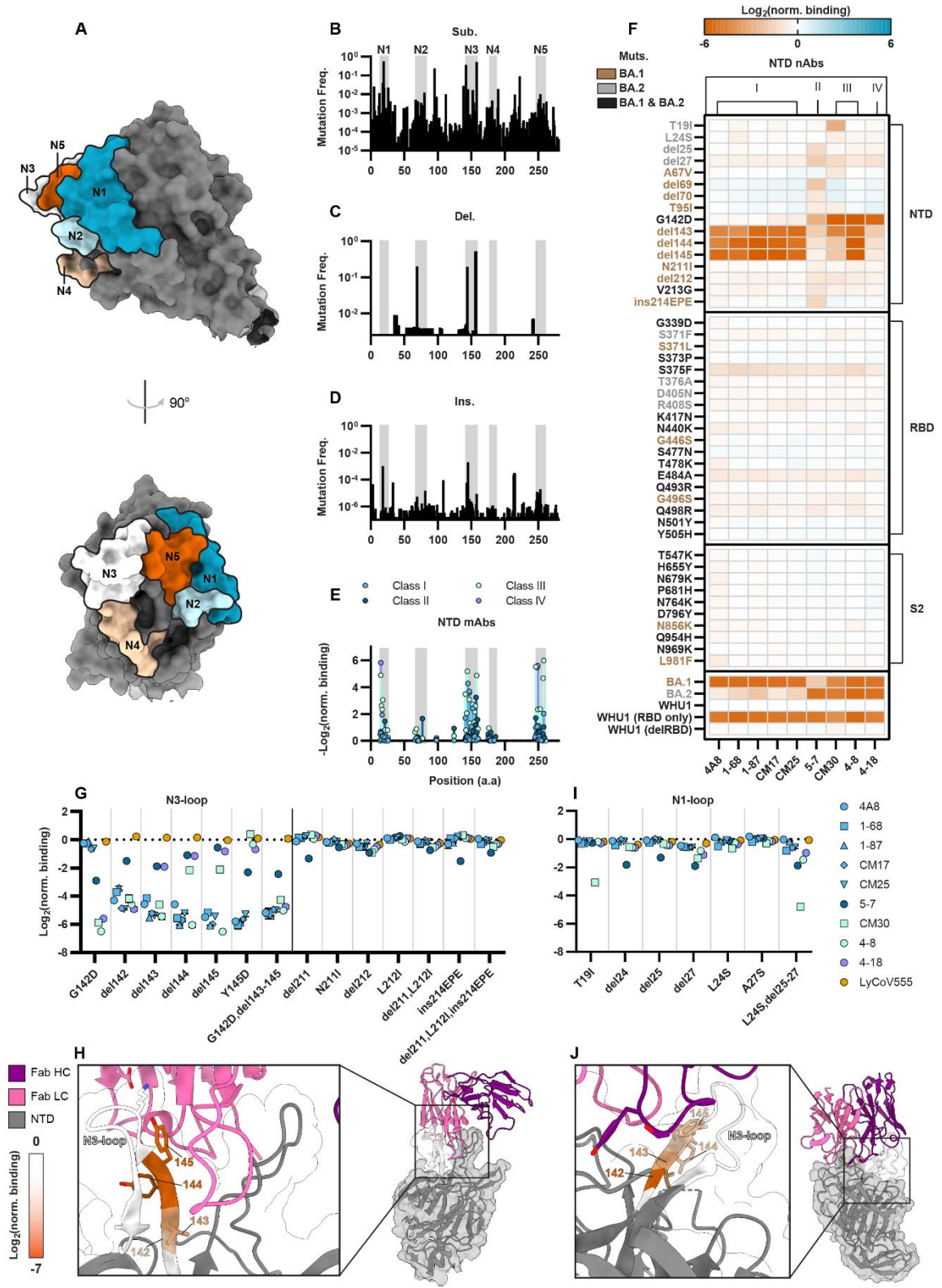


Figure S2. Immunologic selection to evade mAbs at the NTD supersite, Related to Figure 2

- (A) NTD domain structure (PDB: 7DDN (Zhang et al., 2021)) with colored and labeled N-Loops (N1-N5).
- (B-D) Frequency of (B) NTD-substitutions, (C) NTD-deletions, and (D) NTD-insertions (GISAID accessed on 18/December/2021; STAR Methods).
- (E) Spike display binding measurements of single alanine substitutions at each N-loop position. Dots represent mean binding values for each class of mAbs. These data were previously published and reanalyzed for this figure (Javanmardi et al., 2021).
- (F) Binding of NTD-targeting mAbs to WHU1 spikes containing BA.1- and BA.2-mutations normalized to WHU1 spike. Red: decreased binding; blue: increased binding.
- (G) Differences in normalized binding of monoclonal antibodies caused by mutations in the N3-loop and the set of 211-214 mutations found in BA.1. Data represent mean \pm SD of log-transformed values from at least two biological replicates.
- (H) Structure (PDB: 7L2D (Cerutti et al., 2021)) of 1-87 Fab (light chain, pink; heavy chain, violet) in complex with NTD (gray) with highlighted N3-loop (white). Binding data from 1-87 in Fig. S2H is superimposed on the N3-loop.
- (I) Differences in normalized binding of monoclonal antibodies caused by mutations in the N1-loop mutations found in BA.2. Data are a mean \pm SD of log-transformed values from at least two biological replicates.
- (J) Structure (PDB: 7L2E (Cerutti et al., 2021)) of 4-18 Fab (light chain, pink; heavy chain, violet) in complex with NTD (gray) with highlighted N3-loop (white). Binding data from 4-18 in Fig. S2H is superimposed on the N3-loop.

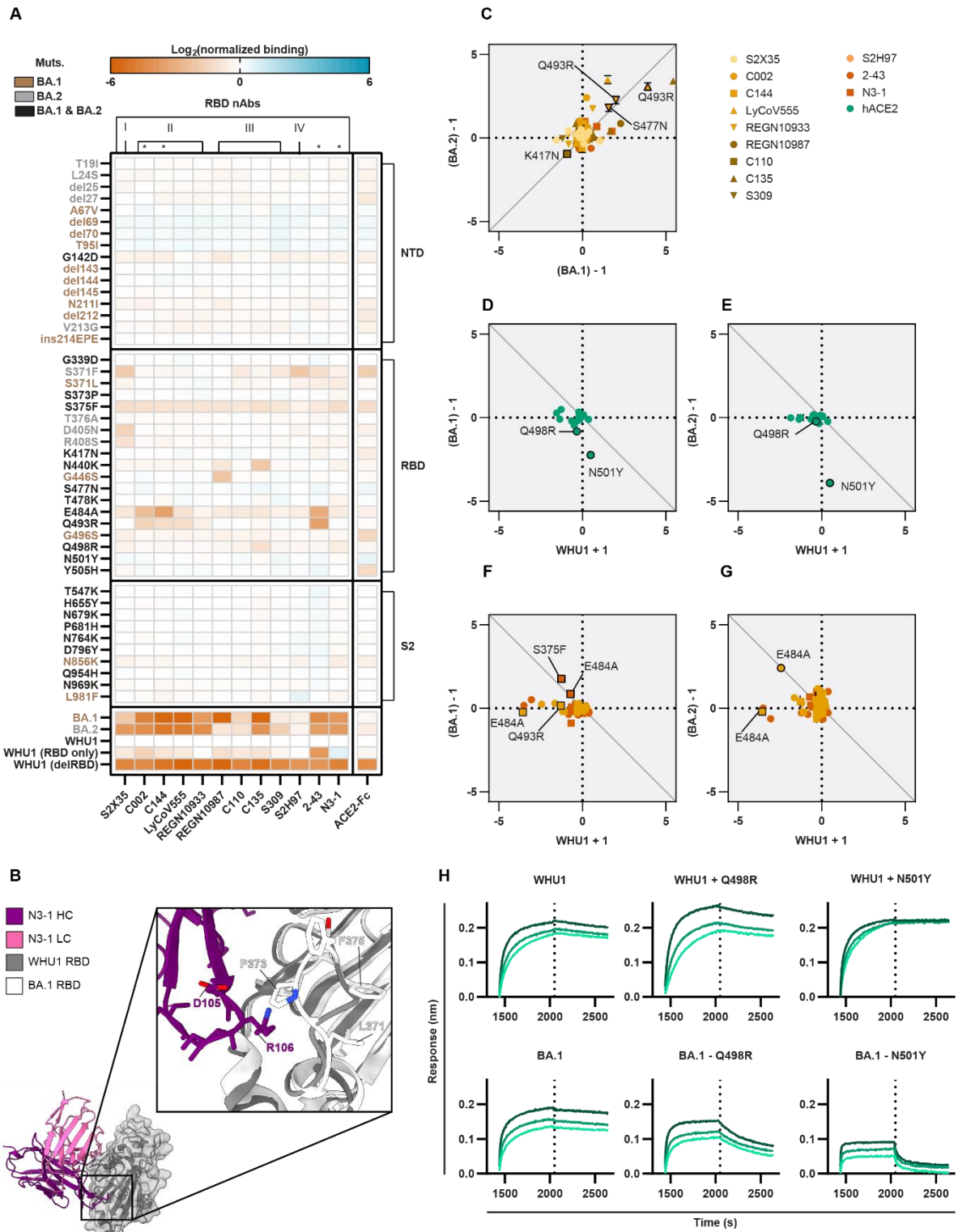


Figure S3. Omicron RBDs broadly escape mAbs while preserving hACE2 affinity, Related to Figure 3

- (A) Relative binding of RBD-targeting mAbs to WHU1 spikes containing BA.1- and BA.2- mutations. Red, decreased binding; blue, increased binding; relative to the WHU1 spike.
- (B) Co-structure of N3-1 (Goike et al., 2021) Fab (light chain, pink; heavy chain, violet) in complex with WHU1 RBD (gray) and BA.1 RBD (white), superimposed. Insert shows zoomed in image of large structural rearrangement in 366-377 hairpin loop of BA.1 RBD and the proximity to N3-1's HC residues.
- (C) Comparison of binding measurements for single amino acid reversions back to the reference (WHU1) amino acids in the BA.1 and BA.2 spikes. Mutations with equal antigenic effects in both spike contexts fall on the diagonal line $y = x$.
- (D) Comparison of the hACE2 binding caused by adding (+1 amino acid substitution) BA.1-RBD mutations to the WHU1 spike versus reverting (-1 amino acid substitution) the corresponding mutations from the BA.1 spike. Mutations with equal antigenic effects in both spike contexts fall on the diagonal line $y = -x$.
- (E) Comparison of the hACE2 binding caused by adding (+1) BA.2-RBD mutations to the WHU1 spike versus reverting (-1) the corresponding mutations from the BA.2 spike. Mutations with equal antigenic effects in both spike contexts are expected to fall on the diagonal line $y = -x$.
- (F) Subset of data from Figure 3E showing mAbs with quaternary binding modes.
- (G) Subset of data from Figure 3F showing mAbs with quaternary binding modes. All data in Figures S3C-G represent mean \pm SD of log-transformed values from at least two biological replicates.
- (H) Biolayer interferometry (BLI) measurements of the on- and off-rate curves for dimeric hACE2-Fc binding spike variants, corresponding to data in Figure 3J.

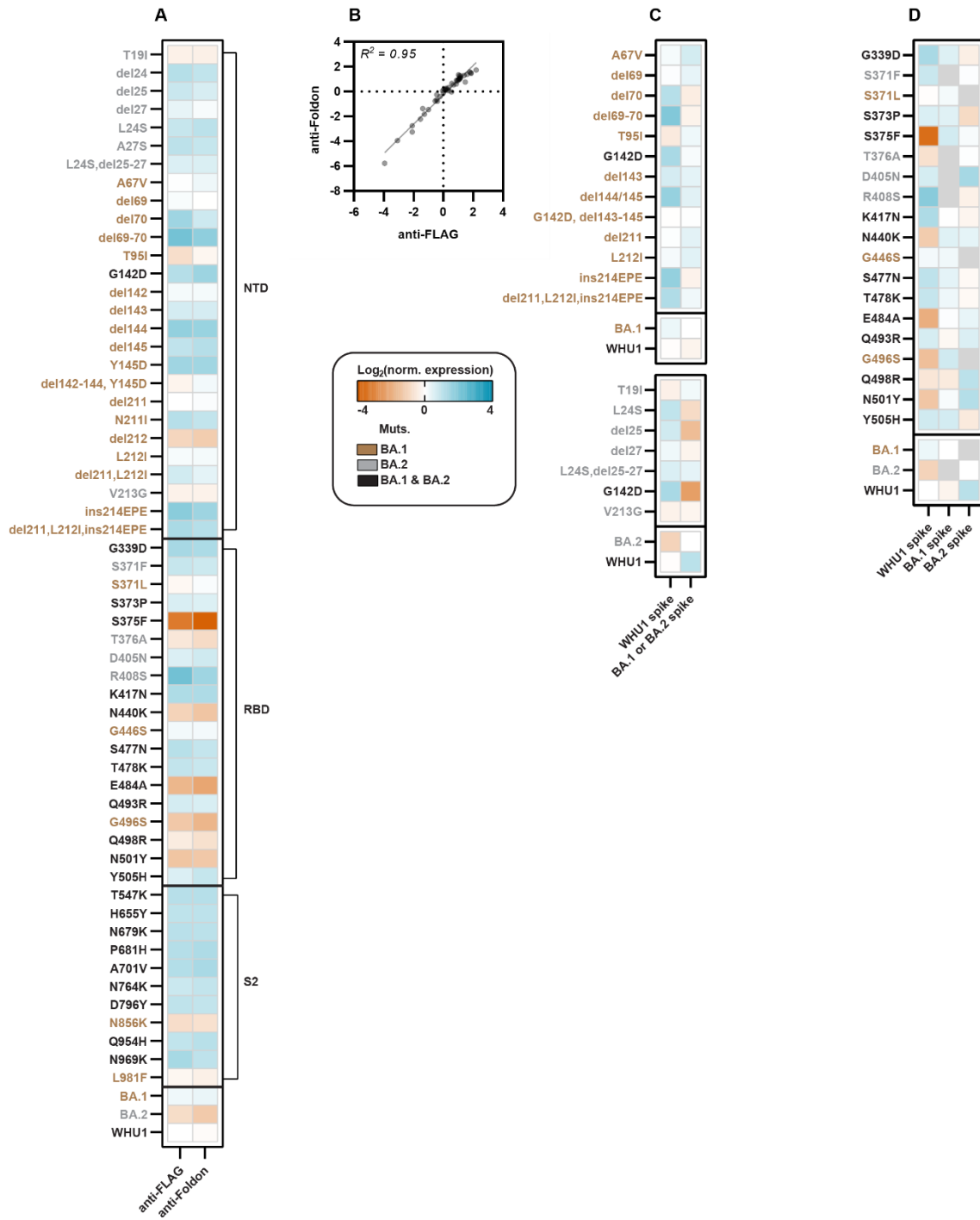


Figure S4. Omicron spike mutations impact spike protein expression, Related to Figure 4

(A) Normalized spike protein expression, measured via anti-FLAG or anti-Foldon, for all BA.1 and BA.2 spike mutations in Figures 2B-E, S2H, S2K, and 3B-D. Red, decreased expression; blue, increased expression, relative to the WHU1 spike protein.

(B) Comparison of anti-FLAG and anti-Foldon expression measurements for all spike variants in A indicates strong correlation between epitopes. Pearson correlation and linear fit shown.

(C) Normalized spike expression values measured for BA.1 (top) or BA.2 (bottom) NTD mutations added to WHU1 spike protein (left column), or reversions of each mutation back to the WHU1 sequence in the BA.1 or BA.2 spikes (right column). Red, decreased expression; blue, increased expression, relative to the WHU1, BA.1 or BA.2 spike proteins, as indicated.

(D) Normalized spike expression values measured for BA.1 and BA.2 RBD mutations added to WHU1 spike (left column), or reversions of each mutation back to the WHU1 sequence in the BA.1 spike protein (middle column) or BA.2 spike (right column). Red, decreased expression; blue, increased expression, relative to the WHU1, BA.1 or BA.2 spike proteins, as indicated.

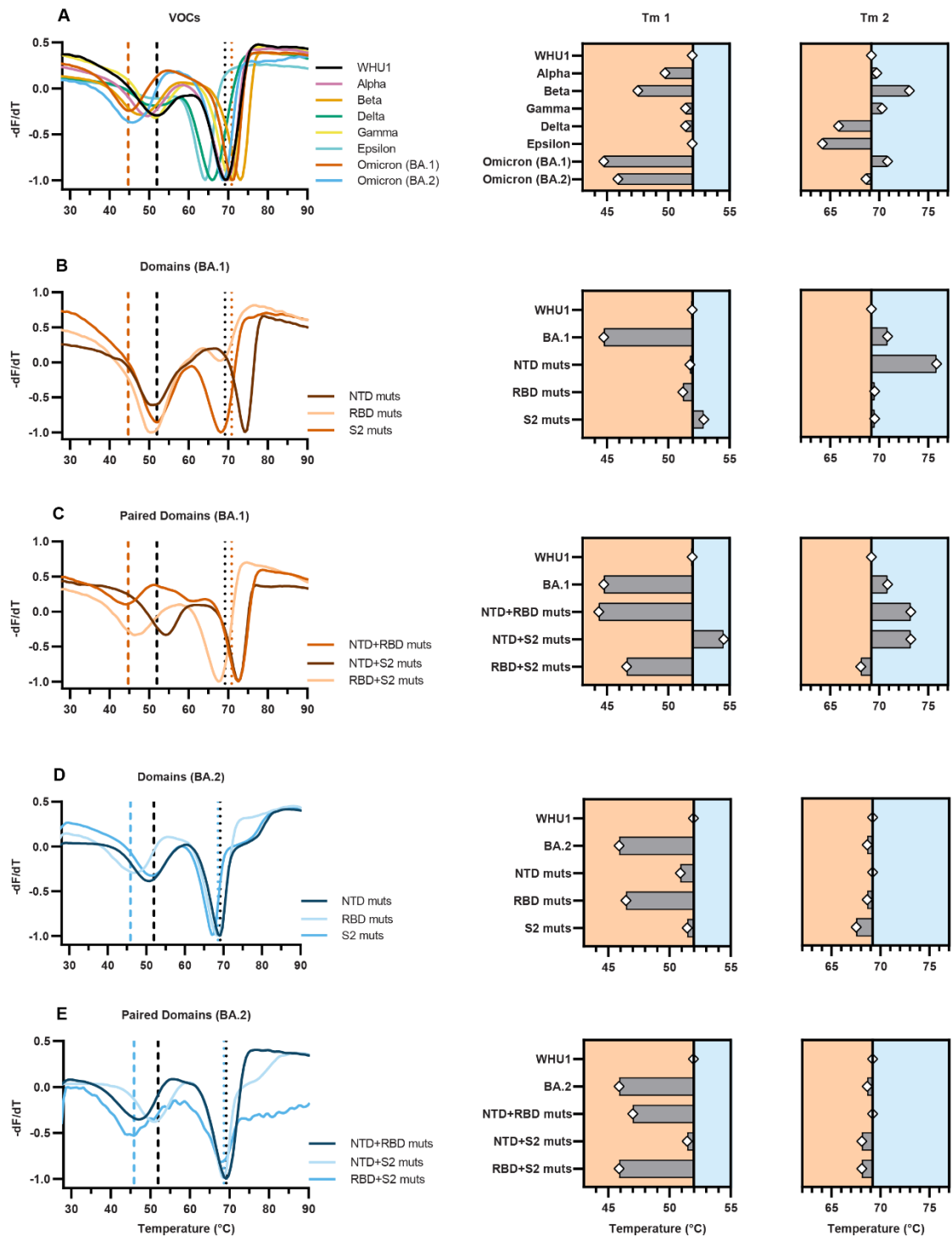


Figure S5. Thermostability measurements of spike protein variants show destabilized Omicron RBD, Related to Figure 4

(A) Differential scanning fluorimetry (DSF) analysis of spike protein thermostability (STAR Methods). First and second melting temperatures ($^{\circ}\text{C}$), T_{m1} and T_{m2} , for WHU1 (black) and BA.1 (red) shown as dotted lines. T_{m1} and T_{m2} reported for each VOC and VOI (right panels). All values shown relative to WHU1, black vertical line.

(B) DSF curves (left) and apparent T_m 's ($^{\circ}\text{C}$) (right) for WHU1 spike proteins containing BA.1-NTD, -RBD, or -S2 mutation sets.

(C) DSF curves (left) and apparent T_m 's ($^{\circ}\text{C}$) (right) for WHU1 spikes containing pairs of BA.1-NTD, -RBD, or -S2 mutation sets.

(D) DSF curves (left) and apparent T_m 's ($^{\circ}\text{C}$) (right) for WHU1 spike proteins containing BA.2-NTD, -RBD, or -S2 mutation sets. First and second melting temperatures, T_{m1} and T_{m2} , for WHU1 (black) and BA.2 (blue) shown as dotted lines.

(E) DSF curves (left) and apparent T_m 's ($^{\circ}\text{C}$) (right) for WHU1 spike proteins containing pairs of BA.2-NTD, -RBD, or -S2 mutation sets.